

Exploring Jet Substructure in Semi-visible jets

Deepak Kar^{a,1}, Sukanya Sinha^{b,1}

¹School of Physics, University of Witwatersrand, Johannesburg, South Africa

Received: date / Accepted: date

Abstract Semi-visible jets arise in strongly interacting dark sectors, where parton evolution includes dark sector emissions, resulting in jets overlapping with missing transverse momentum. The implementation of semi-visible jets is done using the Pythia Hidden valley module to duplicate the QCD sector showering. In this work, several jet substructure observables have been examined to compare semi-visible jets and light quark/gluon jets. These comparisons were performed using different dark hadron fractions in the semi-visible jets (signal). The extreme scenarios where signal consists either of entirely dark hadrons or visible hadrons offers a chance to understand the effect of the specific dark shower model employed in these comparisons. We attempt to decouple the behaviour of jet-substructure observables due to inherent semi-visible jet properties, from model dependence owing to the existence of only one dark shower model as mentioned above.

1 Introduction

Searches for dark matter (DM) particles in colliders have remained unsuccessful so far [1]. Consequently in recent years, some focus has shifted to unusual final states, which are not covered by typical searches at the Large Hadron Collider (LHC). One such final state is termed as semi-visible jets (svj), where parton evolution includes dark sector emissions, resulting in jets interspersed with DM particles [2, 3]. While searches for semi-visible jets are underway in the LHC experiments, the focus of this paper is to probe the viability of such searches in boosted topologies. Rather

than making any specific assumptions about the cross-section of the processes potentially resulting in semi-visible jets, the idea here is to examine if the jet substructure of semi-visible jets can be used to discriminate them from ordinary jets produced by light quarks or gluons. Therefore it is important to note that here we are not focusing on the event selection criteria to obtain a reasonable signal over background ratio in order to discriminate large-radius semi-visible jets. We focus on the more challenging scenario of t-channel production mode of semi-visible jets, where the absence of a resonance mass peak makes identifying the substructure difference more critical.

We start by briefly summarising the idea of semi-visible jets in Sec. 2. Then comparisons between semi-visible jets and ordinary jets are presented in Sec. 3, based on their substructure. The robustness of these differences and the underlying reasons are investigated in Sec. 4, before concluding in Sec. 5. For these studies, the Rivet [4] analysis toolkit was used, with the Fastjet package [5] for jet clustering.

2 Semi-visible jets

Semi-visible jets [6] are hypothetical reconstructed collider objects where the visible states in the shower are Standard Model (SM) hadrons. It is assumed in these scenarios that the strongly coupled hidden sector contains some families of dark quarks which bind into dark hadrons at energies lower than a dark-confinement scale Λ_d . In scenarios where the mediator mass is less than the collision energy, simplistic descriptions of collider phenomenology can be constructed, keeping at bay the extra physics details of the theory, observed at energies greater than collider levels, and irrelevant

^ae-mail: deepak.kar@cern.ch

^be-mail: sukanya.sinha@cern.ch

at the LHC. In t-channel setups (Fig. 1), the mediator interacts with DM and one of the SM quarks, usually simplified models consider the scenario of fermionic DM particle which interacts with SM particles via a scalar mediator coupling only to right-handed quarks. A generic t-channel DM simplified model contains an extension of the SM by two additional fields: a DM candidate (χ) and a mediator (ϕ) which has its fundamental representation in $SU(3)_c$ and the dark gauge group considered in the theory. The dark quarks are the DM degrees of freedom at LHC energies, but at scales probed by direct detection (DD) experiments, the DM degrees of freedom are dark mesons and hence DD rates are highly suppressed for such models since they fall below the neutrino background [3].

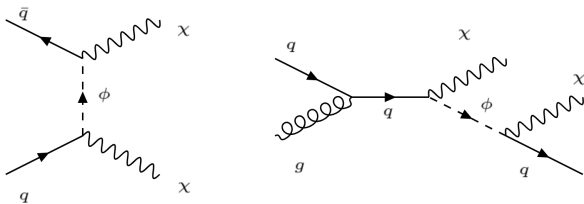


Fig. 1 t-channel setups for DM production.

Considering the approach of parameterising the BSM effects in an EFT expansion, an effective Lagrangian captures all possible interactions:

$$\mathcal{L}_{\text{eff}} = \mathcal{L}_{\text{SM}} + (1/\Lambda)\mathcal{L}_1 + (1/\Lambda^2)\mathcal{L}_2$$

where \mathcal{L}_i are constructed from Standard Model operators that obey the $SU(3)_C \times SU(2)_L \times U(1)$ gauge symmetries, and the higher-dimensional Lagrangian terms representing effective (i.e. non-fundamental) couplings, are suppressed by powers of Λ . As the dark matter particles can appear in the final state of this model, a Dark Matter Effective Field Theory (DMEFT) approach is used, in which the dark matter (DM) is the only additional degree of freedom beyond the SM accessible by current experiments, and hence the interactions of the DM particle with SM particles are described by effective operators (of dimension-6 or higher) of the form:

$$\mathcal{L}_{\text{contact}} \supset (c_{ijab}/\Lambda^2)(\bar{q}_i \gamma^\mu q_j)(\bar{\chi}_a \gamma_\mu \chi_b)$$

Here, the dark sector is a $SU(2)_D$ gauge theory with coupling $\alpha_d = g_d^2/4\pi$, containing two fermionic states $\chi_a = \chi_{1,2}$, and c_{ijab} are $O(1)$ couplings that encode the possible flavour structures, and (assuming minimal flavour-violation) heavy-flavour production channels dominate. The fermions act as dark quarks which interact strongly with coupling strength α_d , similar to QCD. If the mediator is assumed to be unstable, they

will decay to a particle which is charged under a new strong group, but is a singlet under all the SM groups. At the confinement scale Λ_d when α_d becomes non-perturbative, these dark quarks form bound states. [3, 6].

The spectrum of these dark hadronic states have non-perturbative dependencies, and most of the details concerning the spectrum are inconsequential for collider observables. If dark mesons exist, their evolution and hadronization procedure are currently little constrained. They could decay promptly and result in a very SM QCD like jet structure, even though the original decaying particles are dark sector ones; they could behave as semi-visible jets; or they could behave as completely detector-stable hadrons, in which case the final state is just the missing transverse momentum. Apart from the last case, which is more like a conventional BSM MET signature, the modelling of these scenarios is an unexplored area.

In this paper, we consider the case where the final state consists of a jet interspersed with missing transverse momentum (usually referred to as MET) due to a mixture of stable, invisible dark hadrons (with decay time $c\tau > 10$ mm) and visible hadrons from the unstable subset of dark hadrons that promptly decay back to SM particles. The model discussed in [3] uses a simplified parameterisation, where a direct mapping of the Lagrangian parameters to physical observables is not possible since some of the dark sector observables depend on non-perturbative physics. The three parameters of this model are:

- Mass of the scalar bi-fundamental mediator, ϕ
- Dark hadron mass, m_D
- Ratio of the rate of stable dark hadrons over the total rate of hadrons, r_{inv}

The third parameter in its intermediate regime leads to the appearance of semi-visible jets (Fig. 2).

The modelling of such unique final state signatures is done using the Hidden Valley (HV) [8] module of Pythia8 [9], which was designed in order to study a sector which is decoupled from the Standard Model (SM). The basic motivation was the simple idea that one could start with a large number of gauge groups in the high energy limit, but can break them down to fewer groups as the energy decreases, while maintaining the observed cosmological bound. The module tends to achieve a reasonably generic framework for studying BSM models, hence the normal time-like QCD and QED showering has been extended by the addition of the HV sector. HV being a light hidden sector, the associated particles may have masses as low as 10 GeV and the spectrum of the valley particles and

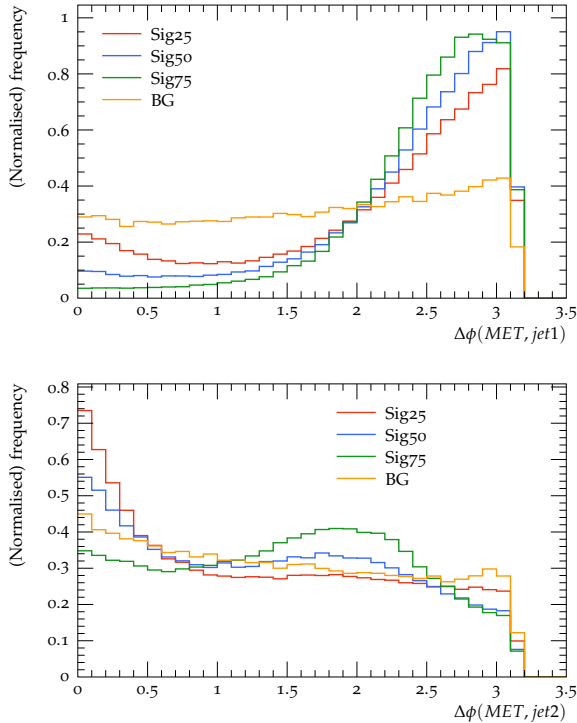


Fig. 3 Distributions of the azimuthal angle difference between the leading (left) and subleading (right) jets with the direction of missing transverse momentum for three different signals corresponding to r_{inv} values of 0.25, 0.50 and 0.75, and the background.

jet. Here we note that even though the svj is more often than not the sub-leading jet, we are mostly interested in differentiating svj from standard quark/gluon-initiated jets, so we can use the leading jet from the background without any loss of generality. It was observed that using only quark or only gluon initiated background jets made no difference.

3.2 JSS observables

Many jet substructure observables have been designed over last decade or so [17, 18], with different sensitivity to different signal jets. In recent works, the focus was on energy correlation observables [19], and discussed the non trivial theoretical uncertainties associated with jet substructure. In this study, we looked at a broad array of observables, Les Houches angularity (LHA) [20], splitting variables r_g and z_g [21, 22], N-subjettiness ratios, τ_{21} and τ_{32} [23], and the ratios of energy correlation functions, C_2 , D_2 , ECF_2 , and ECF_3 [24]. However, we have seen C_2 , LHA and τ_{21} , and τ_{32} were enough to explain most of the features, so we focus on these observables particularly. In general D_2 and ECF_2 were fairly similar, but were less sen-

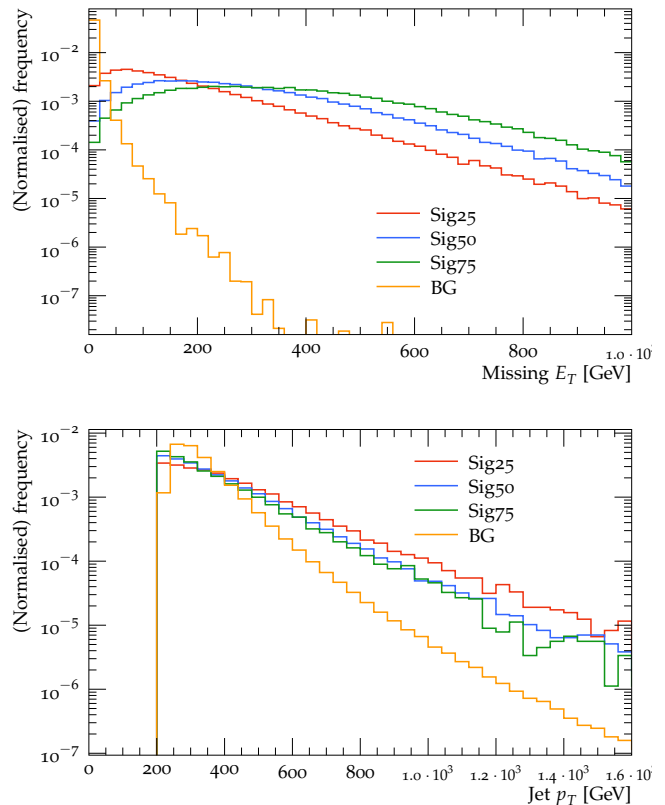


Fig. 4 Distributions of MET (right) and leading jet p_T (left) for three different signals corresponding to r_{inv} values of 0.25, 0.50 and 0.75, and the background.

sitive as compared to C_2 , and ECF_3 , r_g and z_g were mostly insensitive to the effect we are probing.

In order to compare signal and background large-radius jets with similar kinematics, we look at two different jet p_T ranges, 400–600 GeV and 800–1000 GeV, motivated by Fig. 4.

3.3 Results

Distributions of several jet substructure observables are compared between semi-visible and ordinary jets in Fig. 5. The results in p_T range of 400–600 GeV are shown, but the results in the 800–1000 GeV range exhibit the same feature, albeit with a lack of statistics. The distributions are normalised to area, not to cross-section, as we are interested in probing the shape differences.

The overall interpretation is, semi-visible jets result in more multi-pronged substructure, as evidenced in higher values of C_2 and LHA. For τ_{21} , and τ_{32} , the lower values of signal indicate that those are more 2 and 3 pronged respectively, whereas the background is more single pronged. LHA, surprisingly does not show

any difference when changing r_{inv} . For τ , lower values seem closer to background, indicative of the fact that lower dark hadron fraction is indeed more background like. The results here are shown without any theoretical systematic uncertainty. Based on the recent study [19], we can very conservatively assume a 30–40% flat uncertainty on these substructure variables. That would not make the general conclusions arrived at this article invalid, but for certain observables, like τ_{21} for lower r_{inv} values, the discrimination power would be degraded. Also, detector effects can degrade the performance as well, but a quick check using parametrised smearing [25] showed the results we obtain are robust.

4 Understanding the differences

4.1 Model dependence

Currently the only dark shower model that can be used to simulate semi-visible jets is the Pythia8 Hidden Valley module, as discussed in Sec. 2. So an obvious concern is, to what extent the differences seen between signal and background in the previous section is model-dependent. Due to the absence of another model, an unambiguous answer to this question is difficult to arrive at, but considering an extreme scenario of $r_{\text{inv}} = 0$ might offer us some clues. Imposing this condition implies that our signal large-radius jets consist entirely of visible hadrons, and subsequently the behaviour is expected to be like background jets, with low missing transverse momenta, as seen in Fig. 4. However, in this case, requirements on missing transverse momentum magnitude and direction does not really make sense for signal, so for these comparisons, a background-like event selection is employed, assuming leading large-radius jet is the svj.

If the substructure of the signal jets in this case resemble that of the background jets, then that would give us some confidence that the difference seen for non-zero r_{inv} values, as seen before, are caused not only by the model specifications. Among the handles we have on the HV shower, the *HiddenValley:alphaFSR* and the *HiddenValley:pTMin* can be expected to be most consequential. We have found minimal dependence on the latter, but in Fig. 6, we see how the substructure variables change significant with the variation of *HiddenValley:alphaFSR*, where other intermediate values were also probed, but are not shown.

The takeaway message is that in signal jets, C_2 can be made to look similar to background jets for *HiddenValley:alphaFSR* = 0.1. The trend for LHA is not so clear, and it is clear that tau variables are potentially

most sensitive to the HV model implementations, so they will be looked into more carefully as we go along.

While this *HiddenValley:alphaFSR* value is the closest to the QCD α_{FSR} value used in generators, one must note that they cannot be treated at the same footing, as QCD coupling is run at 2-loops. However, based on these results, we will use this *HiddenValley:alphaFSR* value in the rest of the comparisons.

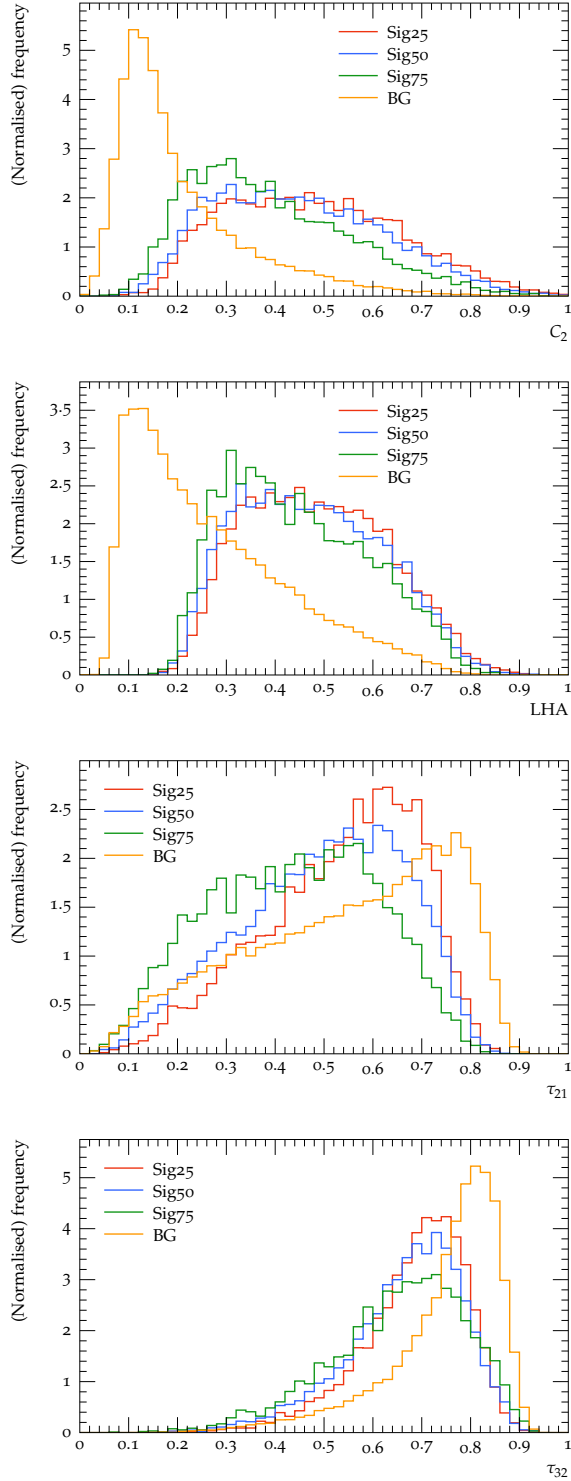


Fig. 5 Comparisons of C_2 (top left), LHA (top right), τ_{21} (bottom left) and τ_{32} (bottom right) between three different signals corresponding to r_{inv} values of 0.25, 0.50 and 0.75, and the background for $\alpha_{FSR} = 1$ and $p_T = 400 - 600$ GeV

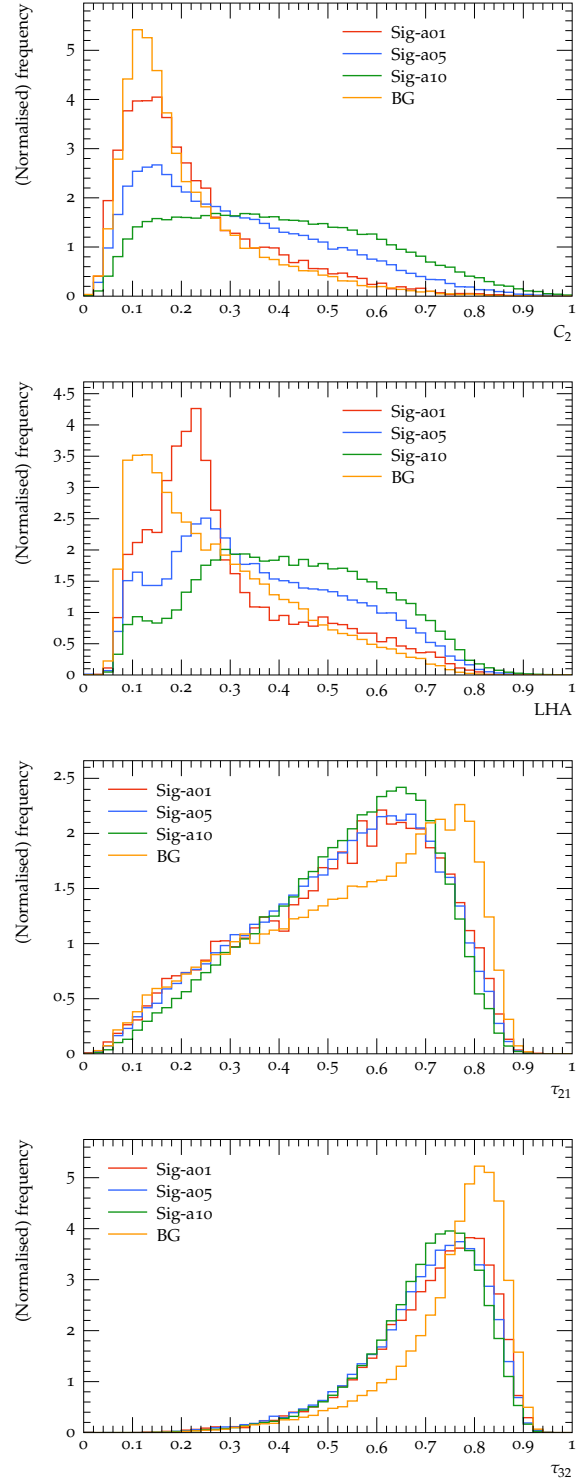


Fig. 6 Comparisons of C_2 (top left), LHA (top right), τ_{21} (bottom left) and τ_{32} (bottom right) between three different signals corresponding to *Hidden Valley: alphaFSR* values of 0.1, 0.5 and 1.0 with $r_{\text{inv}} = 0$, p_T range 400–600 GeV, and the background. It is interesting to note that that a signal with $r_{\text{inv}} = 0$ is not necessarily equivalent to the background.

4.2 Origin of the differences

An understanding of the observed behaviour of jet substructure observables in semi-visible jets is last piece of the puzzle. In order to investigate this, we asked three questions:

1. What is effect of initial state radiation (ISR) and extra radiation on jet substructure?
2. Does decay from intermediate to final dark hadrons affect the substructure?
3. How does grooming affect jet substructure in svj?

In order to answer these, we turn to the other extreme scenario of $r_{\text{inv}} = 1$, which corresponds to the case where the signal jet consists entirely of dark hadrons. Evidently in this case the signal jet itself is ill-defined, but by considering the unphysical scenarios of using dark hadrons in jet clustering, we can try to disentangle several effects.

First, the dark hadrons can be used to form signal jets, along with visible hadrons or without visible hadrons. The extra ME jets and the ISR can be turned off in either case. In each case, the leading large-radius jet is taken, and unless otherwise mentioned, comparisons are performed in the p_T range of 400–600 GeV. Clustering only dark hadron in jets is indicative of the shape an ideal semi-visible jet may result in. We look at the same observables as before in Fig. 7. The more realistic scenario is of course clustering the visible hadrons. In $r_{\text{inv}} = 1$ scenario considered here, the visible hadrons come almost exclusively from ME level extra jets and ISR. Looking at C_2 and τ observables, its clear that adding visible hadrons make the signal jets more multiprong. It is interesting to see how the visible hadrons coming from ISR and ME extra jets affect the substructure differently. Turning off the ISR affects C_2 more than τ observables, perhaps indicating the C_2 is more sensitive to the softer radiation. Additionally turning ME extra jets off has the opposite behaviour, it does not affect C_2 , but makes taus indicative of slightly more two/three pronged substructure. It also implies that ISR adds more activity to semi-visible jets compared to ME extra jets, making them slightly more multi-pronged. Turning off ME extra jets makes the svj produced with less p_T , so that implies we are not comparing the *same* jets in these cases. Surprisingly LHA seem rather insensitive.

An interesting feature can be seen the bottom left τ_{21} distribution of Fig. 7, where two peaks appear. This feature is enhanced for the higher p_T range, and also appears for lower values of *HiddenValley:alphaFSR* as discussed in Sec. 4.1, which can be seen in Fig. 8. This is independent of adding SM hadrons, except when ME extra jets are turned off. This observation is consistent with the occurrence of this feature with

higher p_T , where jets can be more collimated and two-pronged. The lower values of *HiddenValley:alphaFSR* similarly indicate less radiation.

Another sanity check is to examine if the decay from intermediate dark hadrons to the final dark hadrons considered above is responsible for creating or enhancing the substructure. We make the intermediate dark hadrons stable, and cluster them in jets, with and without visible hadrons. In Fig. 9, the comparison of those with the previous results show essentially no difference, except a slightly more flattish shape in lower values of tau for the current case. So it is safe to say the observed substructure is not due to HV decay structure.

The next test was how grooming affects the substructure of semi-visible jets, as grooming preferentially cuts out soft or wide angle radiation. We test the effect of trimming here.

In Fig. 10, we compare different configurations with and without trimming. Trimming in general moves τ_{21} to the left, indicating a cleaner two pronged substructure. This is least pronounced for 'only dark hadron' case, slightly more when visible hadrons are also clustered, and most pronounced for no extra ME jets or ISR case. A comparison between the scenarios of no extra ME jet and no ISR indicates ISR gets more affected by trimming. The same conclusion could also have been reached at looking at C_2 , but the effect was less pronounced. Trimming did not affect the p_T spectra of the signal jets.

Last but not the least, after exploring what effects are not responsible for the specific substructure of semivisible jets, we are ready to answer what is actually responsible. For finite r_{inv} values, only the visible hadrons are clustered in jets in Sec. 3.3, and slightly different substructure were seen for different r_{inv} values. Now, as in Sec. 4.2, if the final dark hadrons are also clustered in the jets, we should expect this difference to go away, as the different amount of *missing* hadrons in each case presumably was responsible for the difference. Indeed, in Fig. 11, we see the expected behaviour. For C_2 , the lines corresponding to the cases where dark hadrons are clustered are almost identical, and while they are not identical for τ_{21} , they lie in between the two original lines. This indicate that the substructure becomes less two-pronged with visible and dark hadrons in them, and the absence of the dark hadrons create the two-pronged structure. These distributions were made with *HiddenValley:alphaFSR* = 1 to have the maximum possible dark radiation.

5 Conclusions

A comprehensive study of the substructure of semi-visible jets has been performed. We demonstrated that a specific hidden valley parameter choice can reduce the model dependence on the Pythia HV module while comparing signal and background jets. The origin of the substructure in semi-visible jet is neither caused by the decay of intermediate dark hadrons, nor by extra ME jets, or ISR, although the latter two affect the substructure. The substructure is created by the interspersing of visible hadrons with dark hadrons. The substructure observables which are least affected by model dependence can be used in searches, and also as inputs to machine learning algorithms trying to identify semi-visible jet via anomaly detection [26]. It must be noted though, that the current model leads to a scenario where kinematic selections like that on missing transverse momentum or leading jet p_T is far more effective in suppressing the background compared to the substructure observables considered here. However, it is not out of the question to have a scenario where kinematic selections still leaves roughly similar signal and background contribution, and then the potential discriminating power of these observables will be more important.

Acknowledgements

DK is funded by National Research Foundation (NRF), South Africa through Competitive Programme for Rated Researchers (CPRR), Grant No: 118515. SS thanks University of Witwatersrand Research Council for Scholarship grant and NRF for grant-holder linked bursary. We thank Tim Cohen and Joel Doss for many useful ideas and suggestions. We also thank Caterina Doglioni, Jannik Geisen, Eva Hansen for many interesting discussions, and for organising the Lund darkjets mini workshop in November 2019, where the authors benefited from discussions with Rikkert Frederix, Stefan Prestel and Torbjörn Sjöstrand. We thank Andy Buckley and Marvin Flores for going over the draft and making relevant suggestions.

References

1. G. Bertone, M. Tait, Tim, Nature **562**(7725), 51 (2018). DOI 10.1038/s41586-018-0542-z
2. T. Cohen, M. Lisanti, H.K. Lou, Phys. Rev. Lett. **115**(17), 171804 (2015). DOI 10.1103/PhysRevLett.115.171804
3. T. Cohen, M. Lisanti, H.K. Lou, S. Mishra-Sharma, JHEP **11**, 196 (2017). DOI 10.1007/JHEP11(2017)196

4. C. Bierlich, et al., SciPost Phys. **8**, 026 (2020). DOI 10.21468/SciPostPhys.8.2.026
5. M. Cacciari, G.P. Salam, G. Soyez, Eur. Phys. J. **C72**, 1896 (2012). DOI 10.1140/epjc/s10052-012-1896-2
6. H. Beauchesne, E. Bertuzzo, G. Grilli Di Cortona, Z. Tabrizi, JHEP **08**, 030 (2018). DOI 10.1007/JHEP08(2018)030
7. E. Bernreuther, F. Kahlhoefer, M. Kr  dmer, P. Tunney, JHEP **01**, 162 (2020). DOI 10.1007/JHEP01(2020)162
8. L. Carloni, T. Sjostrand, JHEP **09**, 105 (2010). DOI 10.1007/JHEP09(2010)105
9. T. Sj  strand, S. Ask, J.R. Christiansen, R. Corke, N. Desai, P. Ilten, S. Mrenna, S. Prestel, C.O. Rasmussen, P.Z. Skands, Comput. Phys. Commun. **191**, 159 (2015). DOI 10.1016/j.cpc.2015.01.024
10. M. Park, M. Zhang, Phys. Rev. D **100**(11), 115009 (2019). DOI 10.1103/PhysRevD.100.115009
11. H. Beauchesne, E. Bertuzzo, G. Grilli Di Cortona, JHEP **04**, 118 (2019). DOI 10.1007/JHEP04(2019)118
12. J. Alwall, R. Frederix, S. Frixione, V. Hirschi, F. Maltoni, O. Mattelaer, H.S. Shao, T. Stelzer, P. Torrielli, M. Zaro, JHEP **07**, 079 (2014). DOI 10.1007/JHEP07(2014)079
13. P. Skands, S. Carrazza, J. Rojo, Eur. Phys. J. **C74**(8), 3024 (2014). DOI 10.1140/epjc/s10052-014-3024-y
14. M.L. Mangano, M. Moretti, R. Pittau, Nucl. Phys. **B632**, 343 (2002). DOI 10.1016/S0550-3213(02)00249-3
15. M. Cacciari, G.P. Salam, G. Soyez, JHEP **04**, 063 (2008). DOI 10.1088/1126-6708/2008/04/063
16. D. Krohn, J. Thaler, L.T. Wang, JHEP **02**, 084 (2010). DOI 10.1007/JHEP02(2010)084
17. R. Kogler, et al., Rev. Mod. Phys. **91**(4), 045003 (2019). DOI 10.1103/RevModPhys.91.045003
18. S. Marzani, G. Soyez, M. Spannowsky, *Looking inside jets: an introduction to jet substructure and boosted-object phenomenology*, vol. 958 (Springer, 2019). DOI 10.1007/978-3-030-15709-8
19. T. Cohen, J. Doss, M. Freytsis, arXiv:2004.00631 (2020)
20. P. Gras, S. H  tche, D. Kar, A. Larkoski, L. L  nblad, S. Pl  tzer, A. Si  dmok, P. Skands, G. Soyez, J. Thaler, JHEP **07**, 091 (2017). DOI 10.1007/JHEP07(2017)091
21. A.J. Larkoski, S. Marzani, G. Soyez, J. Thaler, JHEP **05**, 146 (2014). DOI 10.1007/JHEP05(2014)146

22. ATLAS Collaboration, Phys. Rev. D **101**(5), 052007 (2020). DOI 10.1103/PhysRevD.101.052007
23. J. Thaler, K. Van Tilburg, JHEP **03**, 015 (2011). DOI 10.1007/JHEP03(2011)015
24. A.J. Larkoski, G.P. Salam, J. Thaler, JHEP **06**, 108 (2013). DOI 10.1007/JHEP06(2013)108
25. A. Buckley, D. Kar, K. Nordström, SciPost Phys. **8**, 025 (2020). DOI 10.21468/SciPostPhys.8.2.025
26. E. Bernreuther, T. Finke, F. Kahlhoefer, M. Krämer, A. Majek, arXiv:2006.08639 (2020)

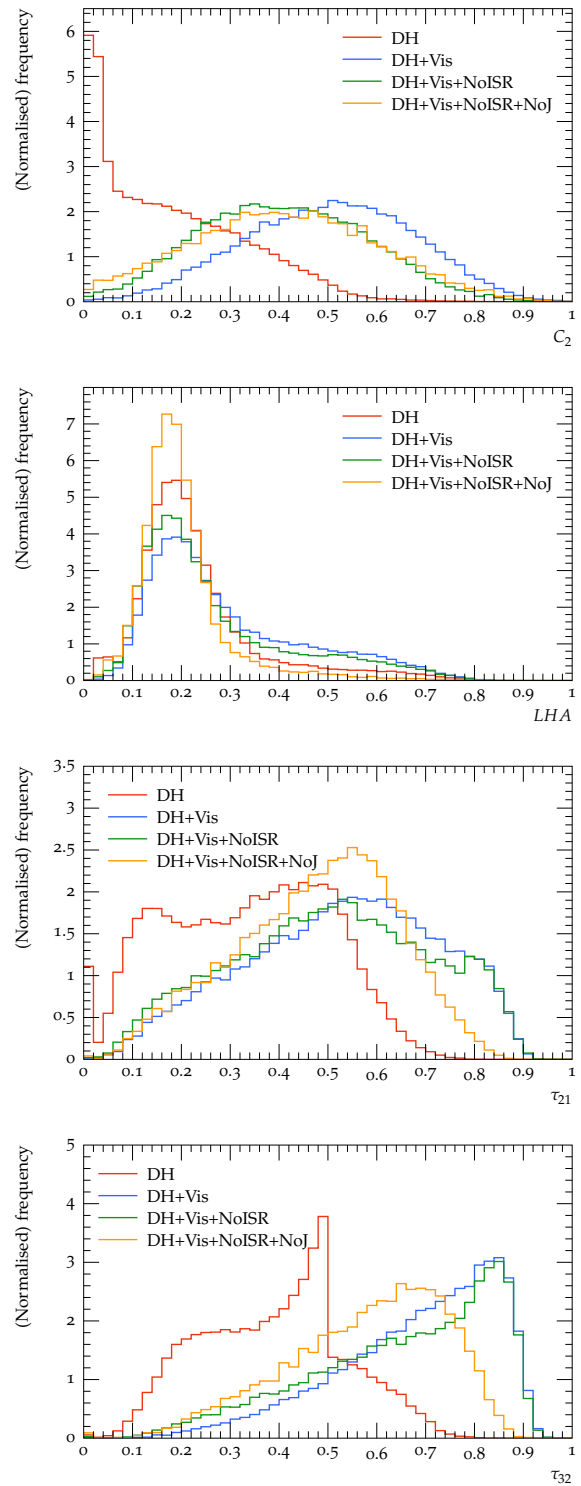


Fig. 7 Comparisons of C_2 (top left), LHA (top right), τ_{21} (bottom left) and τ_{32} (bottom right) between different signals corresponding to clustering only with dark hadrons, adding visible hadrons, tuning ISR off, and also turning extra ME jets off.

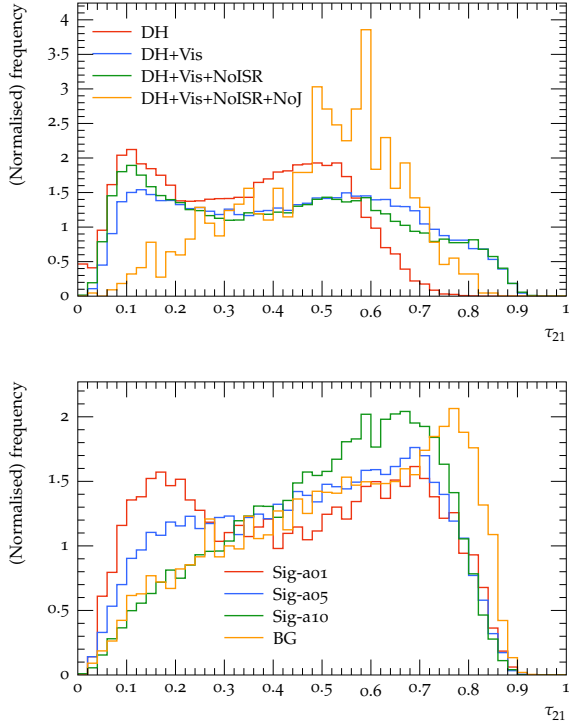


Fig. 8 Comparisons of τ_{21} in jet p_T 800–1000 GeV range between different signals corresponding to clustering only with dark hadrons, adding visible hadrons, tuning ISR off, and also turning extra ME jets off with $r_{\text{inv}} = 1$ (left) and for three different signals corresponding to *HiddenValley:alphaFSR* values of 0.1, 0.5 and 1.0 with $r_{\text{inv}} = 0$ (right).

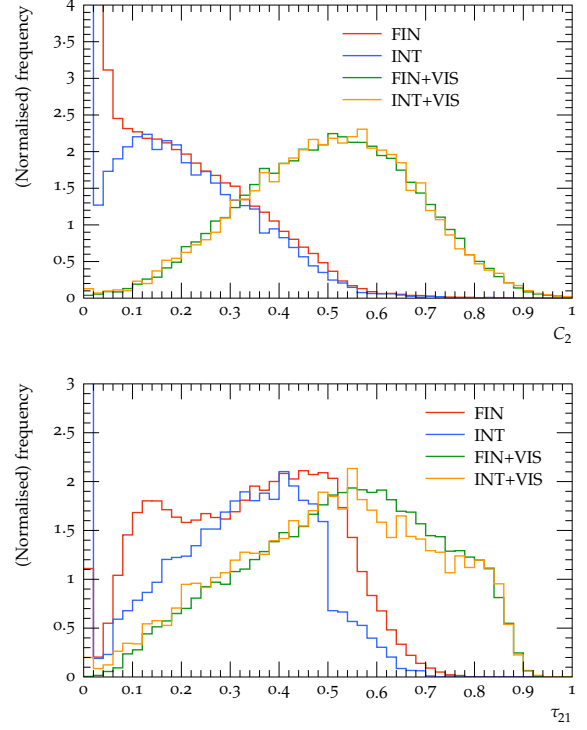


Fig. 9 Comparisons of C_2 (left) and τ_{21} (right) between different signals corresponding to clustering only with final dark hadrons, intermediate dark hadrons and adding visible hadrons in both cases. The entries at zero correspond to cases where the substructure variable could not be calculated.

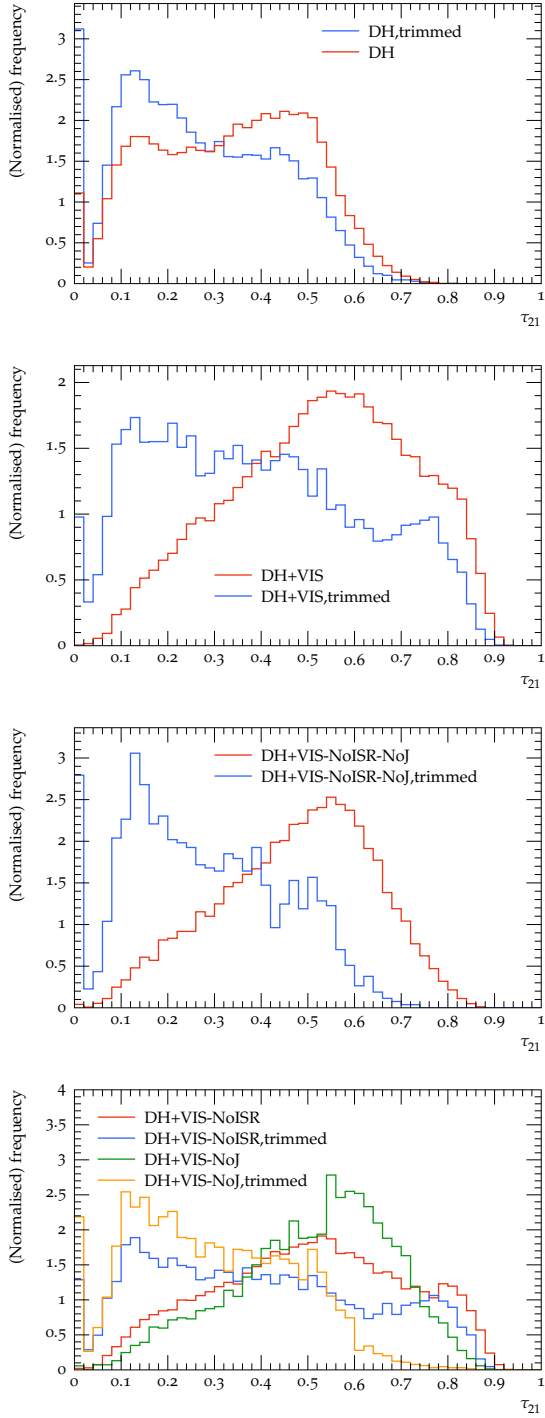


Fig. 10 Comparisons of τ_{21} (right) between ungroomed and trimmed case, for signal configurations corresponding to clustering only with dark hadrons (top left), dark and visible hadrons (top right) turning extra ME jets and ISR off (bottom left) and turning one (but not both) of them off (bottom right). The entries at zero correspond to cases where the substructure variable could not be calculated.

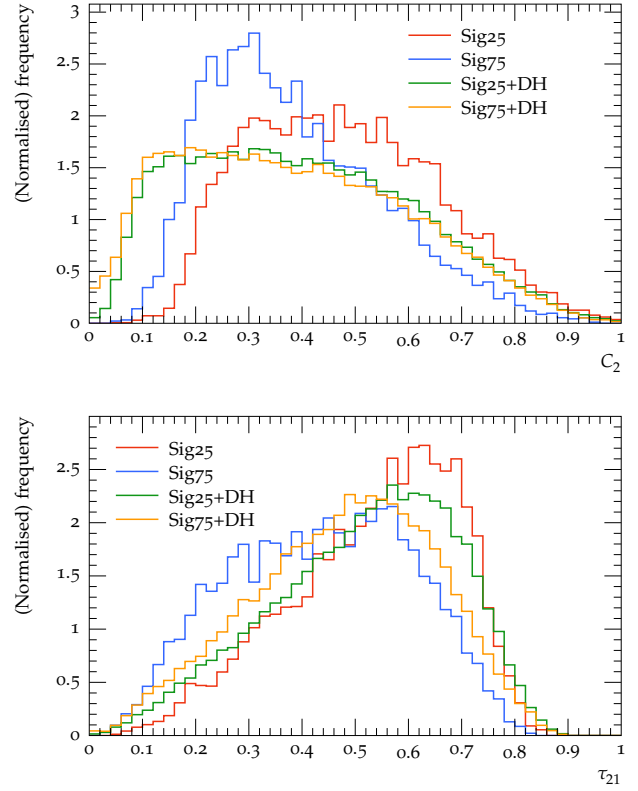


Fig. 11 Comparisons of C_2 (left) and τ_{21} (right) for different signals corresponding to r_{inv} values of 0.25 and 0.75, clustering only the visible hadrons and clustering also with final dark hadrons.